Group 14 Metalloles with Thienyl Groups on 2,5-Positions: Effects of Group 14 Elements on Their π-Electronic Structures†

Shigehiro Yamaguchi, Yujiro Itami, and Kohei Tamao*

Institute for Chemical Research, Kyoto University, Uji, Kyoto 611-0011, Japan

Received May 18, 1998

A series of group 14 metalloles, from silole to stannole, together with cyclopentadiene, having two thienyl groups at the 2,5-positions, have been prepared. Their crystal structures, UV−vis absorption and fluorescence spectra, and cyclic voltammograms have been determined. Theoretical calculations on their electronic structures have also been carried out. On the basis of these experimental and theoretical results, we compared their properties and electronic structures. The group 14 metallole derivatives from silole to stannole have essentially the same electronic structures and, thereby, comparable photophysical properties to each other, while significant differences exist between the cyclopentadiene and silole derivatives. The central group 14 elements, silicon, germanium, and tin, of the metalloles affect the LUMO energy levels of the π-electronic systems to almost the same extent through $\sigma^*-\pi^*$ conjugation.

Introduction

Silole (silacyclopentadiene) is now receiving much attention as a new building unit of π-conjugated systems because of its unique electronic structure.[1−6] Silole has a quite low-lying LUMO level, which is ascribed to the $\sigma^*-\pi^*$ conjugation[7] in the ring, that is, the orbital interaction between the σ^* orbital of the two exocyclic σ bonds on the ring silicon with the π^* orbital of the butadiene moiety, as shown in Figure 1.[8] Based on this electronic structure, silole-containing π-conjugated compounds show unique photophysical properties, such as long-wavelength absorption in their UV−vis absorption spectra.[1,2] For example, 2,5-dithienylsilole **1** has its λ_{max} at 416 nm, which is about 60 nm longer than that of the thiophene trimer, terthiophene (Chart 1).[1a,c] We are now interested in the properties of the π-conjugated systems containing the heavier group 14 metalloles, i.e., germole and stannole, and particularly in the effects of the central group 14 elements on their electronic structures. The heavier central group 14 elements would also play an important role in characterizing the properties through $\sigma^*-\pi^*$ conjugation (vide infra).

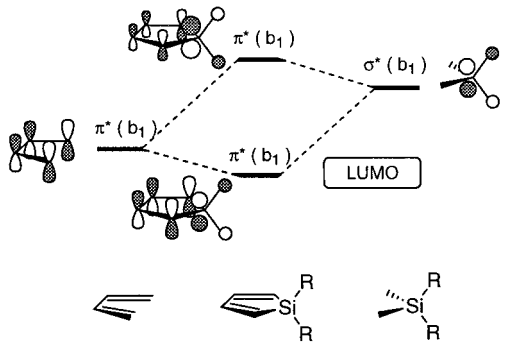

Figure 1. Schematic drawings of $\sigma^*-\pi^*$ conjugation in the LUMO of silole.

Germoles and stannoles, however, have received much less attention as building units for π-conjugated systems. Only 2,5-diphenyl-substituted germoles and stannoles have been reported so far as germole- and stannole-based π-conjugated systems.[9] A comparison of the UV−vis absorption spectra in the series of 2,5-diphenyl-substituted group 14 metalloles has already been made in a recent review article described by Dubac

† Dedicated to Prof. Dr. Edgar Niecke on the occasion of his 60th birthday.

(1) (a) Tamao, K.; Yamaguchi, S.; Shiozaki, M.; Nakagawa, Y.; Ito, Y. *J. Am. Chem. Soc.* **1992**, *114*, 5867. (b) Tamao, K.; Yamaguchi, S.; Shiro, M. *J. Am. Chem. Soc.* **1994**, *116*, 11715. (c) Tamao, K.; Yamaguchi, S.; Ito, Y.; Matsuzaki, Y.; Yamabe, T.; Fukushima, M.; Mori, S. *Macromolecules* **1995**, *28*, 8668. (d) Tamao, K.; Ohno, S.; Yamaguchi, S. *Chem. Commun.* **1996**, 1873. (e) Tamao, K.; Uchida, M.; Izumizawa, T.; Furukawa, K.; Yamaguchi, S. *J. Am. Chem. Soc.* **1996**, *118*, 11974. (f) Tamao, K.; Yamaguchi, S. *Pure. Apple. Chem.* **1996**, *68*, 139. (g) Yamaguchi, S.; Iimura, K.; Tamao, K. *Chem. Lett.* **1998**, 89.

(2) (a) Shinar, J.; Ijadi-Maghsoodi, S.; Ni, Q.-X.; Pang, Y.; Barton, T. J. *Synth. Met.* **1989**, *28*, C593. (b) Barton, T. J.; Ijadi-Maghsoodi, S.; Pang, Y. *Macromolecules* **1991**, *24*, 1257. (c) Chen, W.; Ijadi-Maghsoodi, S.; Barton, T. J. *Polym. Prepr.* **1997**, *38*, 189.

(3) Grigoras, S.; Lie, G. C.; Barton, T. J.; Ijadi-Maghsoodi, S.; Pang, Y.; Shinar, J.; Vardeny, Z. V.; Wong, K. S.; Han, S. G. *Synth. Met.* **1992**, *49*−*50*, 293.

(4) (a) Frapper, G.; Kertész, M. *Organometallics* **1992**, *11*, 3178. (b) Frapper, G.; Kertész, M. *Synth. Met.* **1993**, *55*−*57*, 4255. (c) Kürti, J.; Surján, P. R.; Kertész, M.; Frapper, G. *Synth. Met.* **1993**, *55*−*57*, 4338.

(5) (a) Yamaguchi, Y.; Shioya, J. *Mol. Eng.* **1993**, *2*, 339. (b) Yamaguchi, Y. *Mol. Eng.* **1994**, *3*, 311. (c) Yamaguchi, Y.; Yamabe, T. *Int. J. Quantum Chem.* **1996**, *57*, 73.

(6) (a) Hong, S. Y.; Marynick, D. S. *Macromolecules* **1995**, *28*, 4991. (b) Hong, S. Y.; Kwon, S. J.; Kim, S. C. *J. Chem. Phys.* **1995**, *103*, 1871. (c) Hong, S. Y. *Bull. Kor. Chem. Soc.* **1995**, *16*, 845. (d) Hong, S. Y.; Kwon, S. J.; Kim, S. C.; Marynick, D. S. *Synth. Met.* **1995**, *69*, 701. (e) Hong, S. Y.; Kwon, S. J.; Kim, S. C. *J. Chem. Phys.* **1996**, *104*, 1140.

(7) Bassindale, A. R.; Taylor, P. G. In *The Chemistry of Organic Silicon Compounds*; Patai, S., Rappoport, Z., Eds.; Wiley: New York, 1991; Chapter 14.

(8) Yamaguchi, S.; Tamao, K. *Bull. Chem. Soc. Jpn.* **1996**, *69*, 2327.

(9) Recent reviews for group 14 metalloles: (a) Dubac, J.; Laporterie, A.; Manuel, G. *Chem. Rev.* **1990**, *90*, 215. (b) Colomer, E.; Corriu, R, J. P.; Lheureux, M. *Chem. Rev.* **1990**, *90*, 265.

10.1021/om980393z CCC: $15.00
Publication on Web 10/10/1998

Chart 1

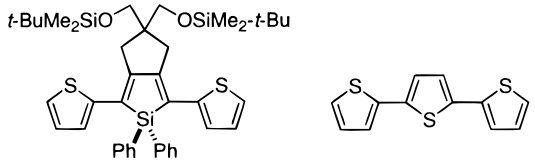

Chart 2

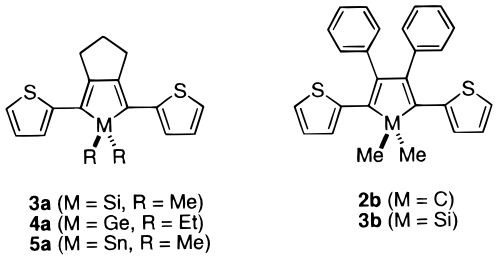

3a (M = Si, R = Me)
4a (M = Ge, R = Et)
5a (M = Sn, R = Me)

2b (M = C)
3b (M = Si)

et al., to show comparable absorption maxima from silole to stannole as well as the shorter absorption maximum of a cyclopentadiene analogue.[9a] However, no information on the origin of these properties and their electronic structures are available. In this context, we investigated in detail the properties of a series of group 14 metalloles, from silole to stannole, together with the cyclopentadiene analogue, having two thienyl groups at their 2,5-positions: hereafter, the term "2,5-positions" will be expediently used also for the "1,4-positions" of cyclopentadienes for simplicity. We now report their synthesis, crystal structures, UV−vis absorption and fluorescence spectra, and electrochemical behavior as well as ab initio calculations. The effects of the central group 14 elements on the π-electronic structures will also be discussed.

Results and Discussion

Syntheses of Thienyl-Substituted Cyclopentadiene (2), Silole (3), Germole (4), and Stannole (5). The compounds prepared in this study are listed in Chart 2. As a series of 2,5-dithienyl group 14 metalloles, we have designed silole **3a**, germole **4a**, and stannole **5a**, which contain bicyclic 3,4-dialkylmetallole rings. The synthetic routes to these compounds are shown in Scheme 1. The silole **3a** was prepared in a manner similar to the procedure reported for the preparation of **1**.[1a,c,10] Thus, 1,7-dithienyl-1,6-heptadiyne **6** was allowed to react with hydrodisilane $HMe_2SiSiMe_3$ in the presence of the $Ni(acac)_2/PEt_3$/DIBAH catalyst system to give **3a** in 25% yield. Compounds **4a** and **5a** were synthesized based on the procedure reported by Fagan and Nugent.[11] Thus, 1,4-dithienylzirconacyclopentadiene **7**, prepared from **6** with $Cp_2ZrCl_2/2n$-BuLi, was allowed to react with Et_2GeCl_2 in refluxing toluene for 60 h. Isolation by silica gel column chromatography gave the germole **4a** in 23% yield. Similarly, the stannole **5a** was obtained in 32% yield by the reaction of **7** with Me_2SnBr_2.

Scheme 1

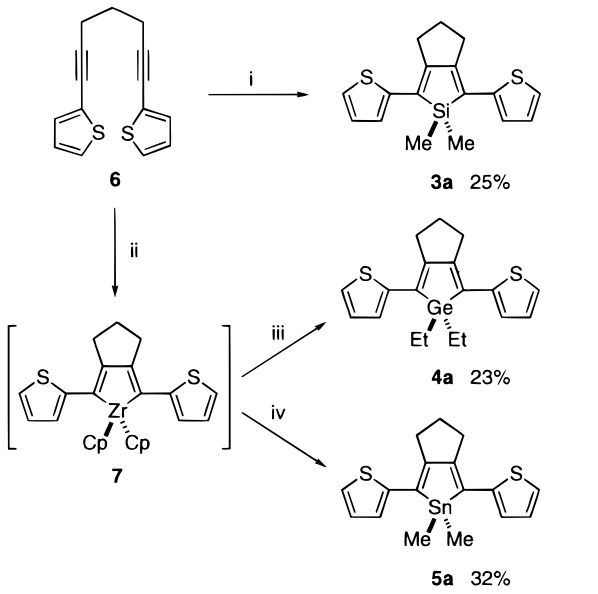

[a] Reagents and conditions: (i) $HMe_2SiSiMe_3$ (2 mol amount), $Ni(acac)_2$ (0.05 mol amount), PEt_3 (0.10 mol amount), DIBAH (0.10 mol amount), THF, reflux, 30 h. (ii) Cp_2ZrCl_2 (1 mol amount), *n*-BuLi (2.2 mol amount), Et_2O, −78 °C to rt, 2 h. (iii) Et_2GeCl_2 (2 mol amount), toluene, reflux, 60 h. (iv) Me_2SnBr_2 (1 mol amount), toluene, reflux, 60 h.

Scheme 2

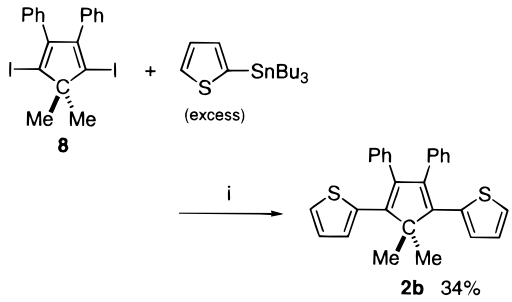

[a] Reagents and conditions: (i) $Pd_2(dba)_3{\cdot}CHCl_3$ (0.05 mol amount), $P(furyl)_3$ (0.10 mol amount), THF/DMF, 80 °C, 12 h.

The synthesis of a carbon analogue having the same skeleton as those of **3a**−**5a** was rather difficult because of a limited number of methodologies for the synthesis of the cyclopentadiene derivatives. Therefore, to evaluate differences between the carbon and silicon analogues, we decided to prepare another series of the dithienylmetalloles, **2b** and **3b**, which have diphenyl-substituted cyclopentadiene and silole skeletons, respectively (Chart 2).

We have recently reported the synthesis of diiodocyclopentadiene **8** based on the intramolecular reductive cyclization of bis(phenylethynyl)methane.[12] The cyclopentadiene **2b** was prepared in 34% yield by the cross-coupling reaction of this diiodide **8** with 2-thienylstannanes in the presence of the $Pd_2(dba)_3{\cdot}CHCl_3/P(furyl)_3$ catalyst system as shown in Scheme 2.[13] The silole **3b** was prepared in 82% yield by a one-pot procedure starting from bis(phenylethynyl)silane **9** based on the intramolecular reductive cyclization using lithium naphthalenide followed by the Pd(0)-catalyzed cross-coupling reaction, as shown in Scheme 3.[1e]

(10) Ni(0)-catalyzed intermolecular cyclization of alkynes with hydrodisilanes: Okinoshima, H.; Yamamoto, K.; Kumada, M. *J. Am. Chem. Soc.* **1972**, *94*, 9263.
(11) (a) Fagan, P. J.; Nugent, W. A. *J. Am. Chem. Soc.* **1988**, *110*, 2310. (b) Fagan, P. J.; Nugent, W. A.; Calabrese, J. C. *J. Am. Chem. Soc.* **1994**, *116*, 1880.
(12) Yamaguchi, S.; Tamao, K. *Tetrahedron Lett.* **1996**, *37*, 2983.
(13) Farina, V.; Krishnan, B. *J. Am. Chem. Soc.* **1991**, *113*, 9585.

Scheme 3

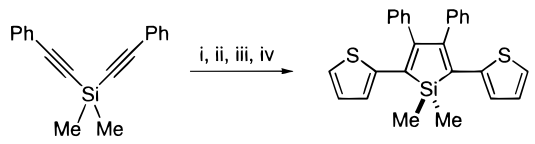

9 **3b** 82%

[a] Reagents and conditions: (i) Lithium naphthalenide (4 mol amount), THF, rt, 5 min. (ii) Ph_3SiCl (2 mol amount), −78 to 0 °C, 1 h. (iii) $ZnCl_2$·TMEDA (2 mol amount), rt, 1 h. (iv) 2-Bromothiophene (2 mol amount), $PdCl_2(PPh_3)_2$ (0.05 mol amount), THF, reflux, 12 h.

Crystal Structures of 2,5-Dithienylmetalloles. Crystal structures of a series of 2,5-dithienyl group 14 metalloles, **3a**, **4a**, and **5a**, have been determined by X-ray crystallography in order to compare their structures. Their crystal data are summarized in Table 1, and the selected bond distances and angles are listed in Table 2. As a representative, the crystal structure of **4a** is shown in Figure 2; for the structures of **3a** and **5a**, see Supporting Information. In all these compounds, the 2,5-thiophene rings have *anti*-coplanar arrangements to the central metallole ring; the twisted angles between the two thiophene mean planes and the metallole mean plane are 6.14 and 10.55° for **3a**, 4.45 and 16.53° for **4a**, and 5.97 and 8.95° for **5a**, respectively. As for the geometries of the central metallole rings, the heavier metalloles have the longer C(1)−M(1) bond lengths accompanied with the smaller C(1)−M(1)−C(4) angles, apparently due to the larger atomic radii of the heavier central group 14 elements. A superimposed view of the metallole rings for these compounds, shown in Figure 3, displays enlargement of the metallole rings by the change in the central elements. As a general structural feature of these metallole rings, it is also noteworthy that the exocyclic M−C(sp^3) bond lengths are shorter than those of the endocyclic M−C(sp^2) bonds in each metallole ring.[14]

Photophysical Properties of 2,5-Dithienyl Group 14 Metalloles. The UV−vis absorption spectra and fluorescence spectra of silole **3a**, germole **4a**, and stannole **5a** are shown in Figures 4 and 5, respectively, and their data are summarized in Table 3, where the data for the 3,4-diphenyl analogues, cyclopentadiene **2b** and silole **3b**, are also included for comparison. Considering the substituent effect on the 3,4-positions, a comparison has been made in two series of compounds, **3a**, **4a**, and **5a**, and **2b** and **3b**, separately. The following features are noted.

(1) The three metalloles, silole **3a**, germole **4a**, and stannole **5a**, have almost the same absorption maxima around 405 nm for the $\pi-\pi^*$ transition with almost the same molar absorption coefficients. This observation is similar to the previously reported results for a series of 2,5-diphenylmetalloles.[9a] On the other hand, in the other series, the absorption maximum of silole **3b** is about 50 nm longer than that of cyclopentadiene **2b**. These results suggest that a large difference in the electronic structure exists between the cyclopentadiene and silole derivatives, but the heavier germole and stannole derivatives have electronic structures similar to those of the silole derivatives.

(2) In the fluorescence spectra, a similar tendency is observed. Thus, a marked difference exists between the cyclopentadiene and the silole. The silole **3b** has its emission maxima about 50 nm longer than that of **2b**. In the series of bicyclic 2,5-dithienylmetalloles, the silole **3a** has a slightly (∼10 nm) longer emission maximum than those of germole **4a** and stannole **5a**. Far more interesting is the variation in the quantum yields of these compounds. Thus, the quantum yield of cyclopentadiene **2b** is seven times higher than that of the silicon analogue **3b**. While the compounds **3a** and **4a** have comparable quantum yields, the quantum yield of stannole **5a** is much lower probably due to the heavy element effect of tin.

Electrochemical Behavior of 2,5-Dithienyl Group 14 Metalloles. The cyclic voltammetry data of the 2,5-dithienylmetalloles are summarized in Table 4. All the redox processes observed for these compounds are irreversible. While the cyclopentadiene **2b** and the silole **3b** have comparable anodic peak potentials (E_{pa}), the cathodic peak potential (E_{pc}) of **3b** is about 0.4 V lower than that of **2b**. On the other hand, the three bicyclic 2,5-dithienylmetalloles, **3a**, **4a**, and **5a**, have comparable E_{pa} and E_{pc} values, again indicating the comparable electronic structures in this series.

Theoretical Study of the Electronic Structures of the 2,5-Dithienyl Group 14 Metalloles. To obtain a deeper insight into the electronic structures of these 2,5-dithienylmetalloles, we carried out ab initio calculations on their model compounds, cyclopentadiene **2c**, silole **3c**, germole **4c**, and stannole **5c** (Chart 3), which have methyl groups on the central Group 14 elements and no substituents on the 3,4-positions of the central metallole rings.[15] The geometries of these compounds were optimized at the DFT/B3LYP level of theory within constraints of the C_{2v} symmetry and *anti*-coplanar arrangements of the three rings. The HOMO and LUMO energy levels calculated at the Hartree−Fock (HF) level for the optimized structures are summarized in Table 5 and plotted in Figure 6.

The calculated HOMO and LUMO energy levels are very consistent with the experimental data determined by the cyclic voltammetry. While the HOMO levels for these four compounds are comparable to each other, there is a noteworthy difference in the LUMO levels between the cyclopentadiene and the silole, maintaining almost the same LUMO levels hereafter. The differences in the LUMO energy levels between **2c** and **3c**−**5c** are 0.25−0.30 eV. The difference between the cyclopentadiene **2c** and the silole **3c** should be ascribed to the σ^*-

(14) This tendency is also shown by the ab initio calculations described in this paper. Thus, the exocyclic M−C(sp^3) and the endocyclic M−C(sp^2) bond lengths (Å) in the optimized structures are as follows, respectively: **3c**, 1.884, 1.897; **4c**, 1.968, 1.978; **5c**, 2.130, 2.129. Interestingly, only the cyclopentadiene **2c** has a longer M−C(sp^3) bond length (1.558 Å) than the M−C(sp^2) bond length (1.546 Å).

(15) Calculations for silole ring systems: (a) Niessen, V.; Kraemer, W. P.; Cederbaum, L. S. *Chem. Phys.* **1975**, *11*, 385. (b) Gordon, M. S.; Boudjouk, P.; Anwari, F. *J. Am. Chem. Soc.* **1983**, *105*, 4972. (c) Guimon, C.; Pfister-Guillouzo, G.; Dubac, J.; Laporterie, A.; Manuel, G.; Iloughmane, H. *Organometallics* **1985**, *4*, 636. (d) Damewood, J. R., Jr. *J. Org. Chem.* **1986**, *51*, 5028. (e) Khabashesku, V. N.; Balaji, S. E.; Boganov, V.; Nefedov, O. M.; Michl, J. *J. Am. Chem. Soc.* **1994**, *116*, 320. (f) Goldfuss, B.; Schleyer, P. v. R. *Organometallics* **1995**, *14*, 1553. (g) Goldfuss, B.; Schleyer, P. v. R.; Hampel, F. *Organometallics* **1996**, *15*, 1755. (h) Goldfuss, B.; Schleyer, P. v. R. *Organometallics* **1997**, *16*, 1543. (i) West, R.; Sohn, H.; Bankwitz, U.; Joseph, C.; Apeloig, Y.; Mueller, T. *J. Am. Chem. Soc.* **1995**, *117*, 11608. (j) Hinchliffe, A.; Soscún M. H. J. *J. Mol. Struct. (THEOCHEM).* **1995**, *331*, 109. See also refs 3−6 and 8.

Table 1. Crystal and Intensity Collection Data for 3a, 4a, and 5a

	3a	4a	5a
empirical formula	$C_{17}H_{18}S_2Si$	$C_{19}H_{22}S_2Ge$	$C_{17}H_{18}S_2Sn$
mol wt	314.53	387.09	405.14
cryst dimens, mm	0.50 × 0.40 × 0.30	0.50 × 0.40 × 0.30	0.50 × 0.40 × 0.30
cryst syst	orthorhombic	monoclinic	orthorhombic
space group	*Pbca* (No.61)	$P2_1/n$ (No.14)	*Pbca* (No.61)
cell const			
a, Å	17.0563(4)	11.8575(9)	17.321(1)
b, Å	21.4661(3)	9.5937(7)	21.403(2)
c, Å	8.6974(2)	16.551(1)	8.9734(4)
β, deg		105.414(6)	
V, Å^3	3183.3999	1815.0699	3326.5801
Z	8	4	8
D_{calcd}, g cm^{-3}	1.312	1.416	1.618
temp, °C	−100	−100	−100
radiation	Mo Kα (*λ* = 0.710 70 Å)	Mo Kα (*λ* = 0.710 70 Å)	Mo Kα (*λ* = 0.710 70 Å)
μ(Mo Kα), cm^{-1}	3.97	19.11	17.75
$2\theta_{max}$, deg	55.2	55.1	55.2
no. of collcd rflcns	3712	3980	3883
no. of unique rflcns	2781 ($I > 4\sigma(I)$)	2960 ($I > 4\sigma(I)$)	2891 ($I > 4\sigma(I)$)
rfln/parameter ratio	15.28	14.80	15.88
R^a	0.054	0.047	0.059
$R_w{}^b$	0.080	0.071	0.086
goodness of fit	1.33	1.25	1.31

[a] $R = \sum||F_o| - |F_c||/\sum|F_o|$. [b] $R_w = [\sum w(|F_o| - |F_c|)^2/\sum\omega F_o^2]^{1/2}$.

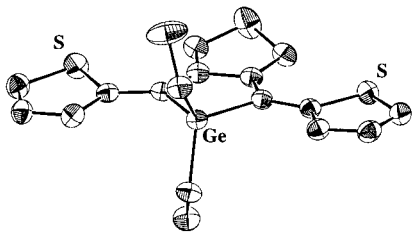

Figure 2. ORTEP drawing of **4a** (50% probability for thermal ellipsoids). Hydrogen atoms are omitted for clarity.

Table 2. Selected Bond Distances and Angles for 2,5-Dithienyl Group 14 Metalloles

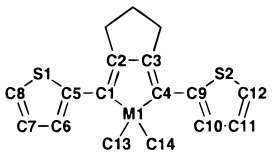

	3a (M = Si)	**4a** (M = Ge)	**5a** (M = Sn)
	Bond Distances (Å)		
M(1)−C(1)	1.887(2)	1.959(3)	2.148(4)
M(1)−C(13)	1.870(2)	1.958(4)	2.127(5)
C(1)−C(2)	1.356(3)	1.351(4)	1.370(6)
C(2)−C(3)	1.473(3)	1.475(4)	1.485(6)
C(1)−C(5)	1.447(3)	1.453(4)	1.435(6)
C(5)−C(6)	1.390(3)	1.372(4)	1.373(7)
C(6)−C(7)	1.419(3)	1.412(4)	1.441(7)
C(7)−C(8)	1.353(4)	1.341(4)	1.359(9)
S(1)−C(5)	1.742(2)	1.736(3)	1.750(5)
S(1)−C(8)	1.721(3)	1.719(4)	1.713(6)
	Bond Angles (deg)		
C(1)−M(1)−C(4)	92.99(8)	89.9(1)	84.6(2)
M(1)−C(1)−C(2)	105.9(1)	106.5(2)	106.8(3)
C(1)−C(2)−C(3)	117.6(2)	119.0(3)	120.6(4)
M(1)−C(1)−C(5)	126.3(1)	124.0(2)	124.5(3)
C(13)−M(1)−C(14)	110.43(9)	110.3(1)	112.0(2)
S(1)−C(5)−C(6)	109.5(1)	109.0(2)	109.7(3)
C(5)−C(6)−C(7)	113.1(2)	114.3(2)	113.6(5)
C(6)−C(7)−C(8)	113.3(2)	112.4(3)	112.0(5)
C(5)−S(1)−C(8)	92.5(1)	92.2(1)	92.4(3)

π^* conjugation in the silole ring according to our previous report.[8] The metalloles **3c**−**5c** have resembling LUMO shapes which have lobes on the central group

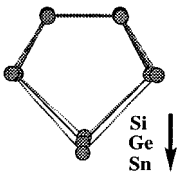

Figure 3. Superimposed view of the metallole rings in the crystal structures of the 2,5-dithienylmetalloles **3a**, **4a**, and **5a**.

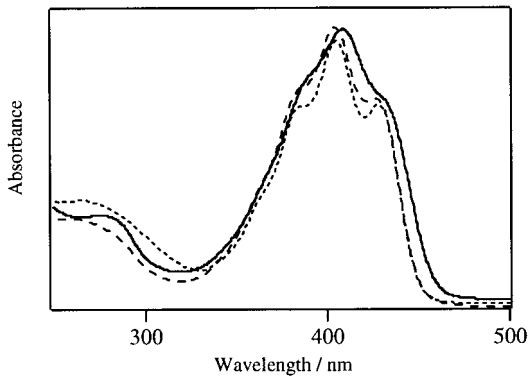

Figure 4. UV−vis absorption spectra of 2,5-dithienylmetalloles in chloroform: **3a**, solid line; **4a**, dashed line; **5a**, dotted line.

14 elements, implying that the $\sigma^*-\pi^*$ conjugation plays an important role also in the germole and stannole analogues.

The corresponding σ^* orbital levels were estimated by the ab initio calculations for Me_2MH_2 (M = C, Si, Ge, Sn), the results being shown in Figure 7. In contrast to a significant difference between the carbon and silicon cases, the σ^* orbital levels are comparable for the silicon and germanium cases, and that of the stannane analogue decreases and becomes close to the π^* orbital level of the π-electronic system. Considering only the energy levels of the σ^* orbital, more effective $\sigma^*-\pi^*$ conjugation would be expected for the heavier metalloles, especially for stannole. However, the present results show comparable LUMO energy levels for the 2,5-dithienylmet-

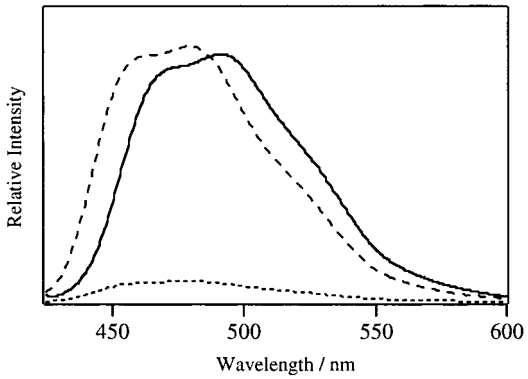

Figure 5. Fluorescence spectra of 2,5-dithienylmetalloles in chloroform: **3a**, solid line; **4a**, dashed line; **5a**, dotted line.

Table 3. UV−Vis and Fluorescence Spectral Data for 2,5-Dithienyl Group 14 Metalloles

	UV−vis[a]		FL[a]	
compound	λ_{max}/nm	log ϵ	λ_{em}/nm[b]	$\Phi_f \times 10^2$ [c]
2b	368	4.10	461	0.996
3b	418	4.28	515	0.141
3a	409	4.38	492	5.44
4a	405	4.37	479	8.72
	428	4.24		
5a	406	4.36	479	0.495
	430	4.24		

[a] In chloroform. [b] Maximum wavelength in emission spectra. [c] Based on quinine sulfate ($\Phi_{366} = 0.55$) as a standard.

Table 4. Electrochemical Data for 2,5-Dithienyl Group 14 Metalloles[a]

compound	E_{pa} [V][b]	E_{pc} [V][b]
2b	+0.60	−2.70
3b	+0.56	−2.29
3a	+0.49	−2.45
4a	+0.49	−2.54
5a	+0.41	−2.52

[a] Determined under the following conditions: Sample, 1 mM; solvent system, *n*-Bu_4NClO_4 (0.1 M) in acetonitrile; Ag/Ag^+ reference electrode; scan rate, 100 mV s^{-1}. Ferrocene was used as a standard. All redox processes are irreversible. [b] Versus Fc/Fc^+.

Chart 3

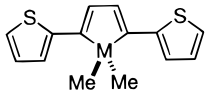

2c (M = C)
3c (M = Si)
4c (M = Ge)
5c (M = Sn)

Table 5. Calculated HOMO and LUMO Energy Levels for 2,5-Dithienyl Group 14 Metalloles[a]

compound	HOMO [eV]	LUMO [eV]
2c	−6.843	1.223
3c	−6.924	0.927
4c	−6.897	0.972
5c	−6.903	0.931

[a] Calculated at the HF//B3LYP level of theory using LANL2DZ basis set, where d polarization functions were added to Si, S, Ge, and Sn.

alloles except for the cyclopentadiene analogue, suggesting a comparable contribution of the $\sigma^*-\pi^*$ conjugation on the LUMO energy levels from silole to stannole. In other words, the $\sigma^*-\pi^*$ conjugation occurs less effectively as the central elements become heavier. This is probably due to the less efficient orbital interaction between the carbon π^* orbital with the σ^* orbital on the central group 14 element having the larger principal quantum number and to the elongated distances between these two orbitals in the heavier metallole rings (Figure 8).

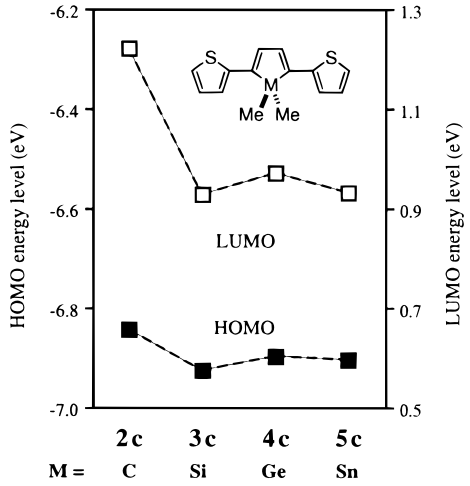

Figure 6. Calculated HOMO and LUMO energy levels of 2,5-dithienylmetalloles at the HF//B3LYP level of theory.

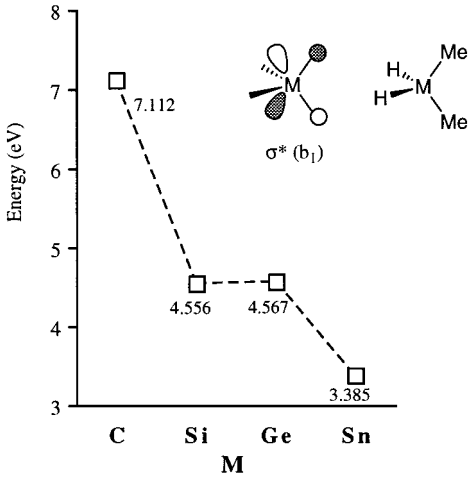

Figure 7. σ^* (b_1) Orbital energy levels of Me_2MH_2 (M = C, S, Ge, Sn) based on ab initio calculations (HF//B3LYP).

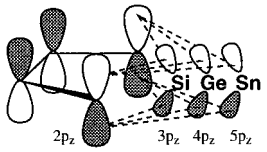

Figure 8. Schematic drawing of the change in $\sigma^*-\pi^*$ conjugation as a function of the central group 14 elements.

Conclusion

We have prepared a series of group 14 metalloles, from silole to stannole, together with cyclopentadiene, having two thienyl groups on the 2,5-positions. Their structures, photophysical properties, electrochemical behavior, and electronic structures have been thoroughly compared. In conclusion, the group 14 metallole derivatives from silole to stannole have essentially the same electronic structures, while a marked difference exists between the cyclopentadiene and silole derivatives. The central group 14 elements, silicon, germanium, and tin, of the metalloles affect the LUMO energy

levels of the π-electron systems to almost the same extent through $\sigma^*-\pi^*$ conjugation. As a consequence, the 2,5-dithienylmetalloles from silole to stannole have comparable absorption maxima in their UV−vis absorption spectra, while the cyclopentadiene analogue has a much shorter absorption maxima. We have recently reported the application of 2,5-diarylsilole derivatives as new efficient electron-transporting emissive materials in organic electroluminescent (EL) devices.[1e] The present results will be informative for the further design of new organic EL materials containing the silole or related ring compounds as a key building unit.

Experimental Section

General. Melting point (mp) determinations were performed using a Yanaco MP-S3 instrument. ^{1}H and ^{13}C NMR spectra were measured with a JEOL EX-270 (270 MHz for ^{1}H, and 67.8 MHz for ^{13}C) spectrometer in C_6D_6 and $CDCl_3$. Chemical shifts are reported in δ ppm with reference relative to the residual protio-solvent (i.e., $CHCl_3$, C_6H_6) peak. UV−visible absorption spectra were measured with a Shimadzu UV-3100PC spectrometer in spectral grade chloroform. Fluorescence spectra were measured with a Perkin-Elmer LS50B spectrometer in degassed spectral grade chloroform. Cyclic voltammograms were measured with a BSA CV-50W. Thin-layer chromatography (TLC) was performed on plates coated with 0.25 mm thick silica gel 60F-254 (Merck). Column chromatography was performed using Kieselgel 60 (70−230 mesh; Merck). High-performance liquid chromatography (HPLC) was done using a 20 mm × 250 mm Wakosil 5Sil column (Wako).

Materials. Diethyl ether (Et_2O) and tetrahydrofuran (THF) were distilled from sodium/benzophenone before use. Other all solvents were dried over appropriate desiccants and distilled under nitrogen. Bis(acetylacetonato)nickel(II) is commercially available and dried in vacuo (100 °C, 0.5 mmHg, 10 h). Triethylphosphine was commercially available. Diisobutylaluminum hydride (DIBAH) was purchased from Aldrich Co., Ltd., as a 1 M hexane solution. 1,7-Di(2-thienyl)-1,6-heptadiyne (**6**) was prepared by the Pd-catalyzed coupling reaction of 1,6-heptadiyne with 2-bromothiophene in the presence of the $PdCl_2(PPh_3)_2$/CuI catalyst in Et_2NH.[16] Pentamethyldisilane $HMe_2SiSiMe_3$ was prepared by the reduction of 1-chloropentamethyldisilane with lithium aluminum hydride in Et_2O. Cp_2ZrCl_2 and Me_2SnBr_2 were commercially available and used without further purification. Et_2GeCl_2 was prepared by chlorination of Et_4Ge using 2.2 molar amounts of acetyl chloride.[17]

1,4-Diiodo-5,5-dimethyl-2,3-diphenylcyclopenta-1,3-diene (**8**) was prepared according to the procedure described in ref 12. All reactions were carried out under a nitrogen atmosphere.

1,1-Dimethyl-3,4-trimethylene-2,5-di(2-thienyl)silole (3a). A nickel(0) catalyst solution was prepared as follows: to a solution of $Ni(acac)_2$ (13 mg, 0.05 mmol) in dry THF (0.5 mL) were successively added PEt_3 (14 μL, 0.1 mmol) and DIBAH (1 M solution in hexane; 0.1 mL, 0.1 mmol) at room temperature. The mixture was then stirred for 30 min. To a mixture of diyne **6** (256 mg, 1 mmol) and $HMe_2SiSiMe_3$ (265 mg, 2 mmol) in dry THF (1.5 mL) was dropwise added the nickel(0) catalyst solution at room temperature. The mixture was refluxed with stirring for 30 h. After confirmation of the disappearance of **6** by TLC and ^{1}H NMR, the solvent was evaporated under reduced pressure. The resulting mixture was passed through a short silica gel column (hexane) and subjected to HPLC on silica gel (hexane/EtOAc = 50/1, R_f = 0.29) to afford 79 mg (0.25 mmol) of **3a** in 25% yield as yellow crystals: mp 175 °C. ^{1}H NMR ($CDCl_3$) δ 0.52 (s, 6H), 2.19 (quintet, J = 7.3 Hz, 2H), 2.71 (t, J = 7.3 Hz, 4H), 6.94−7.06 (m, 6H). ^{13}C NMR ($CDCl_3$) δ −1.94, 26.78, 30.57, 124.31, 124.49, 124.80, 127.33, 143.86, 157.27. UV−vis ($CHCl_3$) λ_{max} nm (log ϵ) 276 (3.90), 380 (sh, 4.21), 409 (4.38), 430 (sh, 4.26). Anal. Calcd for $C_{17}H_{18}S_2Si$: C, 64.91; H, 5.77. Found: C, 64.76; H, 5.71.

1,1-Dimethyl-3,4-trimethylene-2,5-di(2-thienyl)germole (4a). To a mixture of diyne **6** (128 mg, 0.5 mmol) and Cp_2ZrCl_2 (148 mg, 0.5 mmol) in dry Et_2O (1 mL) was added *n*-BuLi (1.60 M hexane solution; 0.69 mL, 1.1 mmol) at −78 °C. The mixture was stirred at the same temperature for 30 min followed by stirring at room temperature for 2 h to form the zirconacyclopentadiene **7** cleanly. After removing the solvents in vacuo, 0.25 mL of dry toluene was added. To this solution was added Et_2GeCl_2 (150 μL, 1 mmol) at room temperature. The mixture was refluxed for 3 days. After confirmation of the disappearance of **7** by ^{1}H NMR, the reaction mixture was diluted with water (20 mL) and extracted with Et_2O (20 mL × 3). The combined organic layer was dried over $MgSO_4$ and filtered. After concentration of the filtrate, the residue was passed through a short silica gel column (hexane/EtOAc = 20/1, R_f = 0.33) and subjected to HPLC on silica gel (hexane/EtOAc = 50/1) to give 45 mg (0.12 mmol) of **4a** in 23% yield as orange crystals: mp 87 °C. ^{1}H NMR (C_6D_6) δ 1.14−1.34 (m, 10H), 1.88 (quintet, J = 7.3 Hz, 2H), 2.66 (t, J = 7.3 Hz, 4H), 6.87−7.00 (m, 6H). ^{13}C NMR δ ($CDCl_3$) 8.30, 9.17, 26.99, 30.57, 124.30, 124.85, 125.21, 127.21, 145.03, 155.76. UV−vis λ_{max} nm (log ϵ) 255 (3.88), 385 (sh, 4.26), 405 (4.37), 428 (4.24). Anal. Calcd for $C_{19}H_{22}GeS_2$: C, 58.95; H, 5.73. Found: C, 58.83; H, 5.74.

1,1-Dimethyl-3,4-trimethylene-2,5-di(2-thienyl)stannole (5a). Zirconacyclopentadiene **7** (1 mmol) was prepared in essentially the same manner as already described. Me_2SnBr_2 (0.31 g, 1 mmol) was added to a dry toluene (1 mL) solution of **7**. The mixture was refluxed for 3 days. After confirmation of the disappearance of **7** by ^{1}H NMR, the reaction mixture was then diluted with water (30 mL) and extracted with Et_2O (30 mL × 3). The combined organic layer was dried over Na_2SO_4 and filtered. After condensation of the filtrate, the residue was passed through a short silica gel column (benzene, R_f = 0.92) and subjected to HPLC on silica gel (hexane/EtOAc = 20/1, R_f = 0.39) to give 127 mg (0.32 mmol) of **5a** in 32% yield as orange crystals: mp 160 °C. ^{1}H NMR (C_6D_6) δ 0.53 (s, $^2J_{H-Sn}$ = 28 Hz, 6H),1.85 (quintet, J = 7.3 Hz, 2H), 2.69 (t, J = 7.3 Hz, 4H), 6.81−7.00 (m, 6H). ^{13}C NMR ($CDCl_3$) δ −6.56 ($^1J_{C-Sn}$ = 152 Hz, 162 Hz), 26.31, 31.77 ($^3J_{C-Sn}$ = 21 Hz), 125.03, 126.60, 126.88, 127.19, 147.19 ($^1J_{C-Sn}$ = 40 Hz), 156.08 ($^2J_{C-Sn}$ = 35 Hz). ^{119}Sn NMR (C_6D_6, Me_4Sn = 0.0 ppm) δ 65.81. UV−vis ($CHCl_3$) λ_{max} nm (log ϵ) 267 (3.96), 385 (sh, 4.23), 406 (4.36), 430 (4.24). Anal. Calcd for $C_{17}H_{22}S_2Sn$: C, 50.40; H, 4.48. Found: C, 50.00; H, 4.43.

5,5-Dimethyl-2,3-diphenyl-1,4-di(2-thienyl)cyclopenta-1,3-diene (2b). A mixture of 1,4-diiodocyclopentadiene **8** (166 mg, 0.34 mmol), 2-thienyltributylstannane (3.0 g, 8 mmol), $Pd_2(dba)_3$·$CHCl_3$ (17.7 mg, 0.017 mmol) and trifurylphosphine (17.1 mg, 0.074 mmol) in 6 mL of THF/DMF = 2/1 mixed solvent was heated at 80 °C with stirring for 8 h. After confirmation of the disappearance of **8** by ^{1}H NMR, the mixture was condensed under reduced pressure. The resulting mixture was passed through a short silica gel column (hexane/EtOAc = 20/1, R_f = 0.50). Recrystallization from EtOAc gave 47 mg of **2b** (0.12 mmol) in 34% yield as pale yellow crystals: mp 210.5−212.5 °C. ^{1}H NMR ($CDCl_3$) δ 1.59 (s, 6H), 6.86−6.92 (m, 4H), 6.99−7.01 (m, 4H), 7.12−7.15 (m, 8H). ^{13}C NMR ($CDCl_3$) δ 23.45, 55.35, 124.82, 126.43, 126.49, 126.90, 127.94, 130.12, 136.01, 137.92, 142.03, 145.23. UV−vis λ_{max} nm (log

(16) Sonogashira, K.; Tohda, Y.; Hagihara, N. *Tetrahedron Lett.* **1975**, 4467.
(17) Sakurai, H.; Tominaga, K.; Watanabe, T.; Kumada, M. *Tetrahedron Lett.* **1966**, 5493.

ϵ) 368 (4.10). Anal. Calcd for $C_{27}H_{22}S_2$: C, 78.98; H, 5.40. Found: C, 78.77; H, 5.29.

1,1-Dimethyl-3,4-diphenyl-2,5-di(2-thienyl)silole (3b). Compound **3b** was prepared in 82% yield by essentially the same procedure described in ref 1e: mp 173 °C. ^{1}H NMR δ 0.69 (s, 6H), 6.85−6.90 (m, 4H), 6.96−7.04 (m, 6H), 7.14−7.20 (m, 6H). ^{13}C NMR δ −1.90, 125.64, 126.18, 126.86, 127.13, 128.45, 129.56, 135.17, 139.05, 142.82, 152.60. UV−vis ($CHCl_3$) λ_{max} nm (log ϵ) 271 (4.04), 291 (sh, 4.02), 418 (4.35). Anal. Calcd for $C_{26}H_{22}SiS_2$: C, 73.19; H, 5.20. Found C, 73.14; H, 5.08.

Cyclic Voltammetry Measurements. These measurements were carried out under the following conditions: Sample, 1 mM; solvent system, *n*-Bu_4NClO_4 (0.1 M) in acetonitrile; glassy carbon working electrode, Pt wire counter electrode, and Ag/Ag^+ reference electrode; scan rate, 100 mV s^{-1}. The observed potentials were corrected with reference to ferrocene added as an internal standard after each measurement.

X-ray Crystal Structure Determination of 3a, 4a, and 5a. Single crystals of **3a**, **4a**, and **5a** suitable for X-ray crystal analysis were obtained by recrystallization from pentane. The intensity data were collected at 173 K on a Rigaku RAXIS−IV imaging plate area detector with graphite-monochromated Mo Kα radiation from a rotating-anode generator operating at 50 kV and 100 mA to a maximum 2θ value of 55°. A total of 22 oscillation images, each being oscillated 3° and exposed for 40 min, 15 oscillation images, each being oscillated 6° and exposed for 40 min, and 10 oscillation images, each being oscillated 6° and exposed for 40 min, were collected for **3a**, **4a**, and **5a**, respectively. The data were corrected for Lorentz and polarization effects and secondary extinction. The crystal structures were solved by direct methods in SIR92,[18] and a full-matrix least-squares refinement was carried out for all non-hydrogen atoms. Hydrogen atoms were included at calculated positions but not refined. All the calculations were performed using the teXsan crystallographic package from the Molecular Structure Corp.

The crystal data and analytical conditions are listed in Table 1. The final atomic coordinates and isotropic temperature factors, and complete lists of bond lengths and angles for all compounds are given in the Supporting Information.

Calculations. Ab initio calculations were carried out with the Gaussian 94[19] program. For all the calculations, the LANL2DZ basis set, which includes both Dunning and Hay's D95 sets for H and C[20] and the relativistic electron core potential (ECP) sets of Hay and Wadt for the heavy atoms,[21] was used and d polarization functions were added to Si, S, Ge, and Sn.[22] Geometry optimizations of all 2,5-dithienylmetalloles were performed using the density functional theory (DFT) with the B3LYP functional[23] under constraints of the C_{2v} symmetry point groups and *anti*-coplanar arrangements between the central metallole rings with outer thiophene rings. Geometries of Me_2MH_2 (M = C, Si, Ge, Sn) were fully optimized also at the DFT/B3LYP level of theory. The orbital energies were obtained by the single point calculations at the Hartree−Fock (HF) level of theory for the optimized structures.

Acknowledgment. We thank Prof. S. Sakaki, Kumamoto University, for helpful discussions about the theoretical calculations. This work was partly supported by Grant-in-Aids (Nos. 07555280 and 09239103) from the Ministry of Education, Science, Sports and Culture, Japan, and by the Japan High Polymer Center.

Supporting Information Available: Crystal structures with atom labels, tables of crystal data and intensity data, atomic coordinates, anisotropic displacement parameters, and bond distances and angles for **3a**, **4a**, and **5a** and tables of optimized geometries for all the calculated compounds (16 pages). Ordering information is given on any current masthead page.

OM980393Z

(18) Altomare, A.; Burla, M. C.; Camalli, M.; Cascarano, M.; Giacovazzo, C.; Guagliardi, A.; Polidori, G. *J. Appl. Crystallogr.* **1994**, *27*, 435.

(19) Frisch, M. J.; Trucks, G. W.; Schlegel, H. B.; Gill, P. M. W.; Johnson, B. G.; Robb, M. A.; Cheeseman, J. R.; Keith, T. A.; Petersson, G. A.; Montgomery, J. A.; Raghavachari, K.; Al-Laham, M. A.; Zakrzewski, V. G.; Ortiz, J. V.; Foresman, J. B.; Cioslowski, J.; Stefanov, B. B.; Nanayakkara, A.; Challacombe, M.; Peng, C. Y.; Ayala, P. Y.; Chen, W.; Wong, M. W.; Andres, J. L.; Replogle, E. S.; Gomperts, R.; Martin, R. L.; Fox, D. J.; Binkley, J. S.; Defrees, D. J.; Baker, J.; Stewart, J. P.; Head-Gordon, M.; Gonzalez, C.; Pople, J. A. *Gaussian 94*; Gaussian, Inc.: Pittsburgh, PA, 1995.

(20) Dunning, T. H., Jr.; Hay, P. J. In *Modern Theoretical Chemistry*; Schaefer, H. F., III, Ed.; Plenum Press: New York, 1976; p 1.

(21) (a) Hay, P. J.; Wadt, W. R. *J. Chem. Phys.* **1985**, *82*, 299. (b) Hay, P. J.; Wadt, W. R. *J. Chem. Phys.* **1985**, *82*, 270. (c) Wadt, W. R.; Hay, P. J. *J. Chem. Phys.* **1985**, *82*, 284.

(22) Höllwarth, A.; Böhme, M.; Dapprich, S.; Ehlers, A. W.; Gobbi, A.; Jonas, V.; Köhler, K. F.; Stegmann, R.; Veldkamp, A.; Frenking, G. *Chem. Phys. Lett.* **1993**, *208*, 237.

(23) Becke, A. D. *J. Chem. Phys.* **1993**, *98*, 5648.